Theor Chem Acc (2009) 124:169–178
DOI 10.1007/s00214-009-0595-z

REGULAR ARTICLE

Ab initio excited states calculations of Kr_3^+, probing semi-empirical modelling

Petr Milko · René Kalus · Ivana Paidarová · Jan Hrušák · Florent Xavier Gadéa

Received: 27 January 2009 / Accepted: 2 June 2009 / Published online: 23 June 2009

Abstract The accuracy of the diatomics-in-molecules (DIM) model for the krypton ionic trimer is examined in a series of ab initio calculations. In the C_{2v} symmetry, the ground states of irreducible representations B_2 and A_1 were calculated using partially spin restricted open-shell coupled cluster method with perturbative triple connections (RHF-RCCSD-T), the relativistic effective core potential (RECP) and an extended basis set of atomic orbitals. Internally contracted multireference configuration interaction method (icMRCI) with the extended and restricted basis set was used to generate the potential energy surfaces (PESs) of the nine electronic states of Kr_3^+ corresponding to $Kr(^1S) + Kr(^1S) + Kr^+(^2P)$ dissociation limit in a wide interval of nuclear geometries. The overall agreement of the accurate ab initio PESs and the diatomics-in-molecules PESs confirms the quality of the DIM Hamiltonian for the Kr_3^+ clusters and justifies its use in dynamical and spectroscopic studies of the Kr_n^+ clusters. Inclusion of the spin–orbit coupling into the ab initio PESs through a semi-empirical scheme is proposed.

Keywords Cluster modelling · Rare gas ions · Ab initio potential energies · Evaporation energies · Spin–orbit coupling · Kr_3^+ · Kr_n^+

P. Milko · I. Paidarová (✉) · J. Hrušák
J. Heyrovský Institute of Physical Chemistry,
ASCR, v.v.i., Dolejškova 3, 182 23 Praha 8, Czech Republic
e-mail: ivana.paidarova@jh-inst.cas.cz

Present Address:
P. Milko
Institute of Organic Chemistry and Biochemistry,
Academy of Sciences of the Czech Republic,
v.v.i., Flemingovo nám. 2, 166 10 Prague, Czech Republic

R. Kalus
Department of Physics, University of Ostrava,
30. dubna 22, 701 03 Ostrava, Czech Republic

F. X. Gadéa
Université Toulouse 3, IRSAMC, LCPQ,
31062 Toulouse, France

1 Introduction

Rare-gas ionic clusters have attracted large attention during the last decades [1]. Although made of identical atoms, the charge is localized in a small strongly bound subunit, and the remaining almost neutral atoms interact through van der Waals and polarization forces. Therefore they are representatives of heterogeneous systems. The investigation of the ionic trimer, aimed in this paper, is essential, because the trimer core is the chromophore in larger clusters. It absorbs the photon excitation and an interesting dynamics follows imprinted by a competition between fission of the core and the evaporation of weakly bound atoms. The internal conversion also plays an important role in the dynamics.

To perform realistic simulations, including photodissociation or more general fragmentation processes, or thermodynamical studies, these systems have been modelled with semi-empirical diatomics-in-molecules (DIM) approaches [2–4] allowing access to many excited states and a simple treatment of the spin–orbit effects important for the heavier rare gases like krypton and xenon [5]. Important advantages of DIM approach are the exact asymptotic behaviour and very low computational expenses. Nevertheless, the semi-empirical origin of the DIM Hamiltonian necessitates justification of the model by ab inito test calculations.

A comprehensive evaluation of the DIM modelling for lighter rare-gas cluster ions was done by Naumkin et al. [6]. They stress that the comparison of the DIM approach with ab initio calculations is most meaningful, when the ab initio PESs are calculated at the same level of theory as the diatomic fragment input data used in the DIM model. Their study covers a large interval of geometries, the RCCSD-T ab initio data for trimers and tetramers are restricted to the lowest states at each symmetry, however. Such evaluations are very useful: a good semi-empirical model built up and applied in a corroboration with reliable ab initio data extends substantially the aptitude of the theoretical tools to describe cluster structures and dynamical processes as it was demonstrated recently by Ritschel et al. [7–9], and it enables to refine the data precision for their use in spectroscopy (F. Merkt, private communication and Ref. [10]).

In this paper, we will consider the complete manifold of the PESs corresponding to the dissociation limit $Kr(^1S) + Kr(^1S) + Kr^+(^2P)$, i. e., nine lowest electronic states involved in the DIM model [4] of the Kr_3^+ system. The evaluation of the semi-empirical model is done in a series of ab initio calculations in a wide interval of nuclear geometries. The paper is organized as follows: First, the diatomics-in-molecules models used in this work are briefly reviewed in Sect. 2. Then, in Sect. 3, the RCCSD-T energies for the ground states are calculated with the same setting as was used for the Kr_2^+ potential energy curves [4], employed as the diatomic fragment input into the DIM model. Finally, in Sect. 4, the RCCSD-T results are used as a benchmark in multireference calculations which necessitate a reduction of the basis set.

2 Diatomics-in-molecules method

The diatomics-in-molecules approach, originally developed by Ellison [11], was applied to rare-gas cluster cations by Kuntz and Valldorf [2] and extended considerably (inclusion of the spin–orbit coupling) by Amarouche et al. [12]. Thenceforth, a number of diatomics-in-molecules studies have been performed for rare-gas cluster cations, including geometric and electronic structure calculations, modelling their photoabsorption, non-adiabatic dynamics or thermodynamical properties (for krypton, see, e.g., Refs. [4, 13–15]). In addition, several detailed descriptions of the methods, including the pioneering papers [2, 12], are available in the literature, and only brief remarks pertinent to the present work are needed here. The reader is referred to the cited papers for further details.

The diatomics-in-molecules approach is based on an expansion of the overall electronic Hamiltonian of the system studied into diatomic and atomic terms [11],

$$\hat{\mathrm{H}} = \sum_{k=1}^{n-1} \sum_{l=k+1}^{n} \hat{\mathrm{H}}_{kl} - (n-2) \sum_{k=1}^{n} \hat{\mathrm{H}}_{k}, \tag{1}$$

where n is the number of atoms involved. If an appropriate basis set of electronic wave functions is used, the elements of the corresponding Hamiltonian matrix can be calculated in terms of the electronic energies of atomic and diatomic fragments only. For example, for an n-atom singly ionized rare-gas cluster (neon–xenon), a basis set consisting of $3n$ valence-bond Slater determinants, $|\Phi_{kp_m}\rangle$ (where $k = 1, \ldots, n$ and $m = x, y, z$), representing states with the positive charge localized in the valence p_m-orbital of atom k, was proposed by Kuntz and Valldorf [2] leading totally to $3n$ wavefunctions for a general cluster size and reducing to nine wavefunctions in the special case of the ionic krypton trimer. Eigevalues of the corresponding 9×9 Hamiltonian matrix represent then the lowest nine energies of the ionized trimer. Below, we denote this simplest interaction model by an acronym DIM.

The original DIM model suffers from a serious drawback, however, since it neglects the spin–orbit (SO) interaction. Such negligence may be acceptable for the lighter rare gases, neon and argon, but cannot be justified for heavier atoms such as krypton. As shown in Ref. [12], the SO coupling can be easily (and reliably) included in the DIM model via a semi-empirical, atoms-in-molecules approach due to Cohen and Schneider [16]. Despite the fact that only atomic SO contributions, arising from the ionic monomer fragment of the trimer, are taken into account the method has been validated many times as extremely accurate for cationic clusters of rare gases, including krypton [4]. Noteworthy, the basis set of electronic wavefunctions to be employed in this case (and, consequently, the dimensionality of the corresponding Hamiltonian matrix) is twice as large as for the DIM model. Simply because two orientations of the spin of the removed electron are to be taken into account. Then, $|\Phi_{kp_m\sigma}\rangle$ (where $k = 1, \ldots, n$, $m = x, y, z$, and $\sigma = \pm 1/2$) represents the electronic state with the positive charge localized in the valence (p_m, σ) spin–orbital of the k-th atom. For trimer a 18×18 Hamiltonian matrix is to be used within the extended model providing in general nine doubly degenerate eigenvalues corresponding to the nine lowest electronic energies, each doubly degenerate. In this work, we denote the DIM model with the inclusion of the SO coupling by DIM + SO.

Another extension of the original DIM model introduced in Ref. [12], namely the inclusion of leading three-body forces (induction terms representing the induced dipole-induced dipole interactions), is used only occasionally in this work, models DIM + ID–ID and DIM + SO + ID–ID, as, for the ionized trimer, does not represent a

substantial improvement of the DIM and DIM + SO models, respectively (cf. Fig. 3 and Table 4).

The diatomics-in-molecules models used in the present work require several independent inputs, namely, (a) the potential energy curves for the electronic ground state and three lowest excited states of the ionic dimer, Kr_2^+, and for the electronic ground state of the neutral dimer, Kr_2, for building up the DIM model, (b) the spin–orbit coupling constant for Kr^+ for including the SO corrections and (c) the static polarizability of the krypton atom for adjusting the ID–ID terms within the DIM + ID–ID and DIM + SO + ID–ID models.[1] In this work we use the state-of-the-art ab initio curves for the ionic krypton dimer taken from Ref. [4], a highly accurate semi-empirical pairwise potential for Kr_2 taken from Ref. [17], the spin–orbit coupling constant taken from Ref. [18] and the static polarizability volume of krypton atom from Ref. [19].

3 RCCSD-T potential energy surfaces in C_{2v} symmetry

The coupled-cluster single- and double-excitations with perturbative estimation of the triplet contributions based on the restricted Hartree–Fock solution (RHF-RCCSD-T) [20–22] and the program package MOLPRO [23] were used for the calculation of the lowest electronic states in each irreducible representation of the C_{2v} point group, B_2, A_1, B_1 and A_2. In the same way as in the calculation of the potential energy curves of Kr_2^+ [4], the inner shell electrons (argon core) have been treated by using relativistic effective core potential (RECP) developed for the Kr atom by Nicklass et al. [24] and corresponding core polarization potential (CPP). The valence electrons (two s and six p on each atom) were treated explicitly with the (hereafter called *extended*) basis set of (10s8p6d6f2g)/[8s6p6d6f2g] Gaussian type atomic orbitals of Ref. [4]. It is the basis set of Niclass et al. [24], reproducing accurately the dipole polarizability, ionization potential and excitation energies of Kr atom in RECP calculations, augmented for a better description of interaction energies by two s, two p and two g orbitals [25, 4].

From the four states, B_2, A_1, B_1 and A_2, only the lower ones, B_2 and A_1, become the ground state in certain region of nuclear configurations. The global minimum $E_{\min} = -54.9248$ a.u. is located at $\alpha = 180°$ and $R = 5.355$ a.u. of the B_2 state. The PESs of the B_2 and A_1 states are represented in Fig. 1 (upper and lower part, respectively) as the functions of the bond distance $R_{12} = R_{23} = R$ and the angle $\alpha(Kr_1–Kr_2–Kr_3)$. For more lucidity of contour diagrams the energies are given in eV with the zero value at the global energy minimum. For geometries with angle $\alpha < 60°$ the B_2 state lies under the A_1 state. At the equidistant (D_{3h}) geometries the two states intersect (conical intersection) and in the region with α from 60° to approximatively 90° depending on R, where the two surfaces cross again (accidental crossing), the A_1 becomes the ground state. For larger α the symmetry of the ground state is B_2.

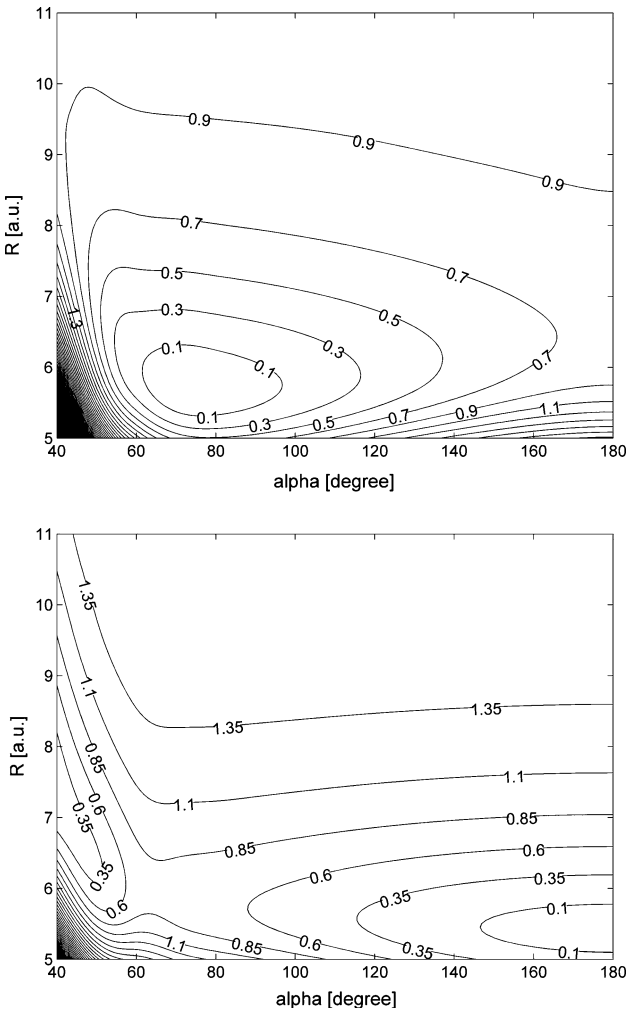

Fig. 1 RCCSD-T contour-line diagram of the potential energy functions for the B_2 (*upper part*) and A_1 (*lower part*) states of Kr_3^+ in C_{2v} geometry. Energies are in eV with zero value corresponding to the global minimum ($E_{\min} = 0$) at $\alpha = 180°$ and $R = 5.355$ a.u. of the B_2 state

The very accurate RCCSD-T energies can be used as a severe test of the potential energy surfaces provided by the semi-empirical DIM model built up from the ab initio potential energy curves of the four lowest Kr_2^+ states

[1] Atomic energies arising from the atomic terms of Eq.1 need not be considered for the following reason. If we identify zero of the energy of Kr_3^+ with the energy of the fully dissociate state, $Kr^+(^2P) + Kr(^1S) + Kr(^1S)$, with the spin–orbit coupling in Kr^+ neglected, the atomic terms will sum up to zero within the DIM model, while correct energy shifts of the two fine-structure states of the ionic monomer, $Kr^+(^2P_{3/2})$ and $Kr^+(^2P_{1/2})$, are provided, at the same time, by the Cohen–Schneider procedure within the DIM + SO model.

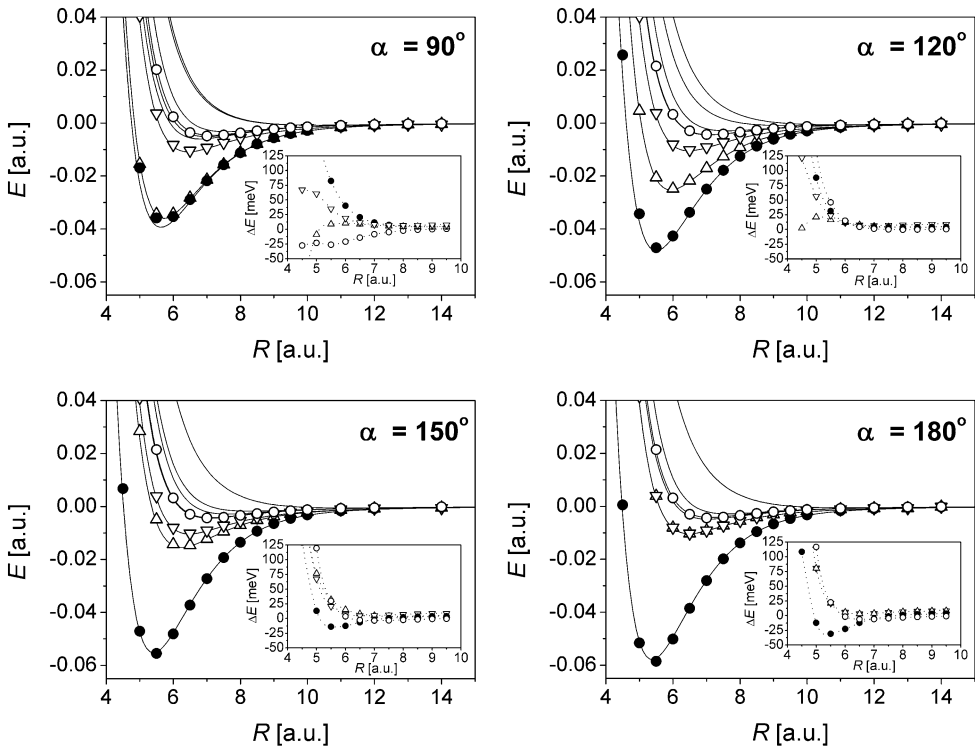

Fig. 2 Comparison of the DIM model (*lines*) with the ab initio RCCSD-T potential energy surfaces for B_2 (*filled circle*), A_1 (*open triangle*), B_1 (*open inverted triangle*) and A_2 (*open circle*) states of Kr_3^+ in selected C_{2v} geometries. Insets show differences between the DIM and the ab initio potentials

calculated at the same level of theory [4] as the RCCSD-T triatomic PESs. The comparison for several representative C_{2v} nuclear geometries is shown in Fig. 2, together with the differences between the DIM and the ab initio potentials reported in insets. They are usually less than a few tens of meV and rise only at very short distances.

The angular dependence of the C_{2v} PESs for a fixed bond, R = 5.5 a.u., shown in Fig. 3 illustrates conical intersections of the $A_1 - B_2$ (and the $B_1 - A_2$) states at $\alpha = 60°$. The intersection occurring in the vicinity of $\alpha = 90°$ is not implied by the symmetry (accidental intersection) and therefore its position depends on the method, and as it is shown in inset of Fig. 3, the DIM and ab initio data slightly differ.

3.1 Spin–orbit interaction

As mentioned above, the spin–orbit (SO) interaction plays an important role and has to be incorporated into the DIM model for heavier Rg_n^+ clusters. In this work it is done according to the Cohen–Schneider scheme [16] as suggested in Ref. [12]. This model, called DIM + SO, was recently used in simulations of the photodissociation process of krypton clusters [5, 26, 27] and enabled the interpretation of the experimental production of atomic ion fragments in the excited fine structure states [28]. In order to compare ab initio energies with the complete DIM + SO model, we have added semi-empirical SO contributions to RCCSD-T energies:

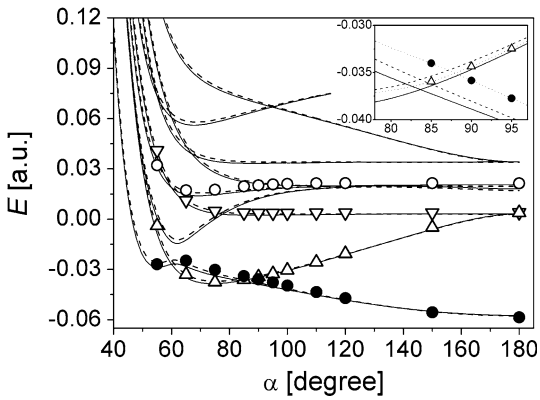

Fig. 3 Comparison of the semi-empirical DIM (*full lines*) and DIM + ID–ID (*dashed lines*) with ab initio RCCSD-T potential energy surfaces for B_2 (*filled circle*), A1 (*open triangle*), B1 (*open inverted triangle*) and A2 (*open circle*) states at C_{2v} arrangement with $R_{12} = R_{23}$ = 5.5 a.u. Detail view of accidental crossing of the B_2 and A_1 states in the vicinity of $\alpha = 90°$ shown in the inset demonstrates that, contrary to conical intersection at $\alpha = 60°$ determined by symmetry, the position of accidental intersection depends on the method and does not coincide for semi-empirical and ab initio data. *Dotted lines* in the inset connecting the ab initio data are added to guide the eyes

$$E_{\text{abinitio+SO}} = E_{\text{abinito}} + E_{\text{DIM+SO}} - E_{\text{DIM}}. \quad (2)$$

The DIM + SO and ab initio RCCSD-T surfaces with the spin–orbit included via Eq. 2 are shown in Fig. 4, where the semi-empirical spin–orbit contributions are shown in insets. Obviously owing to (2) the same agreement between

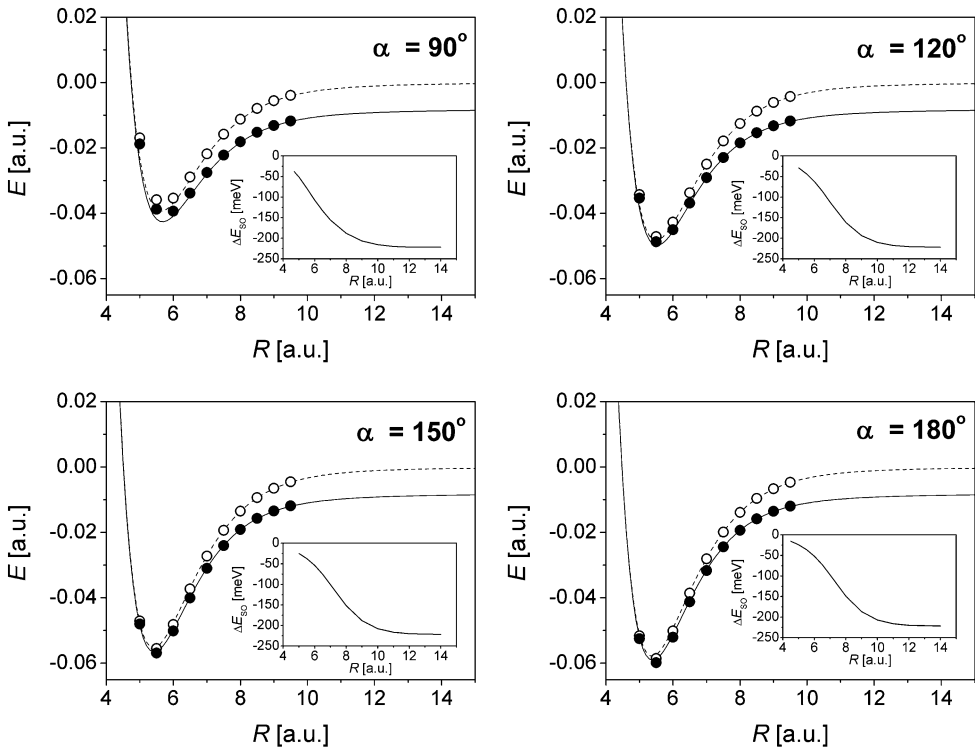

Fig. 4 Inclusion of the spin–orbit coupling via DIM scheme to the RCCSD-T PESs for the ground state of Kr_3^+ in C_{2v} symmetry (*filled circle*) together with spin-free RCCSD-T (*open circle*), DIM (*dashed lines*) and DIM + SO (*full lines*) PESs. The size of the SO corrections is shown in insets

semi-empirical DIM and ad inition results as in Fig. 2 is achieved.

4 icMRCI potential energy surfaces for excited electronic states of Kr_3^+

Although highly accurate, the RCCSD-T treatment is restricted to the ground states of each irreducible representation of symmetry group, and if we wish to have the potential energy surfaces of all nine spin-free electronic states dissociating to $Kr^+(^2P) + Kr(^1S) + Kr(^1S)$, a multiconfiguration method has to be used. We have chosen the internally contracted multiconfiguration interaction (icMRCI) method of Werner and Knowles [29, 30] incorporated in the MOLPRO (version 2006.1) suite of programs [23], because the method offers an efficient and balanced way of treating multiconfiguration effects in the whole region of interatomic separations for both the electronic ground and excited states. Within the icMRCI approach, including all singly and doubly excited configurations relative to the reference configurations, the effect of higher excitations on the PESs has been assessed by the multireference analog of the Davidson correction [31, 32]. From the nine considered electronic states of Kr_3^+, six belong to A′ and three to A″ irreducible representation of the C_s point group used in all our calculations in order to preserve identical active space for higher and lower symmetries. Similarly as in the RCCSD-T treatment, only 23 valence electrons were correlated explicitly, the same RECP, CPP and *extended* basis set as described in the previous section were used. The orbitals for the CI calculations were derived from multiconfiguration self-consistent field (MCSCF) solutions obtained in six- and three-state-averaged complete-active-space SCF (CASSCF) calculations [29, 30, 33, 34] with active space consisting of 12 valence orbitals and starting from the RHF calculation on the neutral trimer. The last choice is crucial for obtaining smooth and continuous potential energy surfaces for all states.

Sample cuts through the PESs of the all states of Kr_3^+ correlating asymptotically to $Kr^+(^2P) + Kr(^1S) + Kr(^1S)$ for C_{2v} ($\alpha = 110°$) and linear symmetric geometries are plotted in Fig. 5. They show a very good agreement between the icMRCI and RCCSD-T results (when available) as well as a satisfactory agreement for all the nine and six icMRCI and DIM potential energy curves for C_{2v} and linear symmetric configurations, respectively. Note, that in the linear symmetric configurations there are three (Π) states that are degenerate.

With the reference active space provided by the preceding CASSCF calculations (12 active orbitals, 6 and 3 CSF's) about 20 and 12 millions of internally contracted configuration are generated in the icMRCI within A′ and A″ symmetry, respectively, leading to impracticable long calculations. Typically one icMRCI point (six A′ and three A″ states) requires about 12 h CPU, while the corresponding RCCSD-T calculation (one state in each irreducible

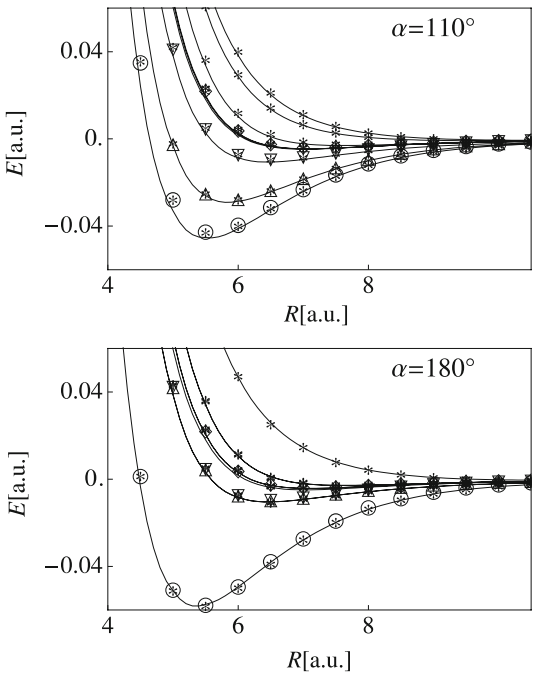

Fig. 5 Comparison of one-dimensional cuts through potential energy surfaces of Kr_3^+ in C_{2v} ($\alpha = 110°$) (*upper part*) and linear symmetric (*lower part*) arrangements calculated in the icMRCI with *extended* basis set (*asterisk*), semi-empirical DIM (*lines*) and RCCSD-T (B_2 *open circle*, A_1 *open triangle*, B_1 *open inverted triangle* A_2 *diamond*) treatments

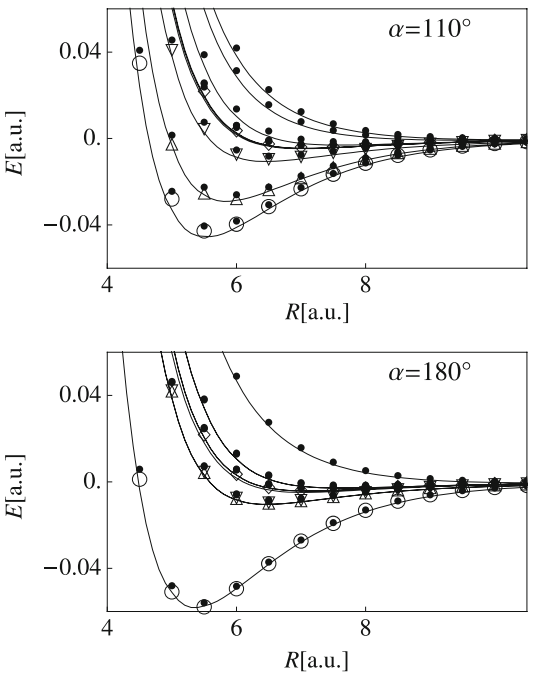

Fig. 6 Comparison of one-dimensional cuts through potential energy surfaces of Kr_3^+ in C_{2v} ($\alpha = 110°$) (*upper part*) and linear symmetric (*lower part*) arrangements calculated in the icMRCI with *reduced* basis set (*filled circle*), semi-empirical DIM (*lines*) and RCCSD-T (B_2 *open circle*, A_1 *open triangle*, B_1 *open inverted triangle* and A_2 *diamond*) treatments

representation) takes about 40 min in parallel calculations on 4× CPU Opteron 3GHz computers. The ab initio results with the *extended* basis set are evidently the most suitable for evaluation of the DIM model constructed of diatomic Kr_2^+ potential energy curves calculated [4] with the identical *extended* basis set, because, as argued by Naumkin et al. [6] in their comparative study the agreement between DIM and ab initio PESs is the closest when the diatomic input data are calculated at the same level of theory as the polyatomic PESs. Moreover, it was observed several times (see, e.g. [35]) that for the rare-gas ions the quality of the DIM model follows the quality of ab initio diatomic data used for its construction. On the other hand, the icMRCI calculations with the *extended* basis set would not be feasible for a larger number of nuclear configurations. An attempt is undertaken to achieve the quantitatively correct results with a smaller basis set which should allow to generate ab initio points in a broad interval of geometries at a reasonable computational cost.

4.1 Reduced basis set

We start with the basis set of Nicklass et al. [24], (8s8p3d1f)/[6s6p3d1f], corresponding to the RECP for the krypton atom. In the same way as in Ref. [4], we have augmented the basis set by one g orbital, with exponent 0.3, optimized in the CI calculation with the aim to get maximum correlation energies of the Kr_2^+ ground state both at the equilibrium and at the asymptotic nuclear configurations. With this (hereafter called *reduced*) basis set, the icMRCI calculations are approximatively 15 times faster than the calculations with the *extended* basis set and can be done for many nuclear configurations. A sample comparison of the icMRCI with *reduced* basis set and the DIM results is presented in Fig. 6.

Figures 5 and 6 evince that the energies obtained in the icMRCI treatment with *reduced* and *extended* bases differ. On the other hand, it is interesting to observe that the excitation energies $\Delta E_i = E_i - E_1, \quad i = 2,...9$, provided by the two approaches are quite close as illustrated for sample geometries in Fig. 7. For bond lengths R greater than 4.5 a.u., the differences between the excitation energies obtained with *extended* and *reduced* bases are only about a few meV, statistical means over all states decrease from 5 meV at R = 4.5 a.u. to 0.7 meV at R = 10 a.u. For R = 4 a.u. the mean is 8 meV at linear symmetric and 300 meV at C_{2v} nuclear configuration, with the maximum value 650 meV. Additional comparative calculations to those presented in Fig. 7 were done in many other nuclear arrangements, they all confirmed very nice agreement of excitation energies obtained in the both icMRCI treatments.

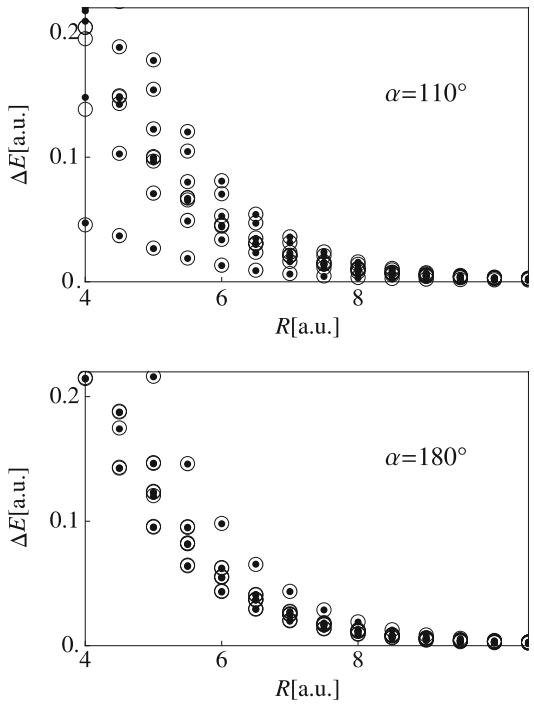

Fig. 7 Comparison of the potential energy differences (transition energies) $\Delta E_i = E_i - E_1, \quad i = 2,...9$ for electronic states of Kr_3^+ in selected C_{2v} ($\alpha = 110°$) and linear symmetric arrangements obtained in the icMRCI with *reduced* (*filled circle*) and with *extended* (*open circle*) basis set calculations

4.2 Multireference ab initio vis-a-vis DIM potential energy surfaces for the nine Kr_3^+ states

In order to obtain accurate ab initio data for all states of Kr_3^+ at a reduced computational cost, we suggest, on the basis of findings of the Sect. 1, to take as the ground state the PES provided by the single-root (RCCSD-T) with *extended* basis set calculations (A′ state in C_s). The PESs for the excited states are then constructed as the sums of the RCCSD-T ground state energies and the excitation energies ΔE_i obtained in the multi-root (icMRCI) calculations with *reduced* basis set.

In Fig. 8 (left column) we demonstrate for selected isosceles and linear symmetric geometries, how such ab initio PESs compare with the DIM model based on the ab initio diatomic data obtained with *extended* basis set. The differences between the ab initio and corresponding DIM energies (right column) show quite satisfactory agreement—with the exception of very short distances, they are smaller than tens of meV.

Another test of the quality of the DIM model is the comparison of charge distributions calculated by DIM and icMRCI methods in Table 1. Again a satisfactory agreement is observed. Note that all multireference calculations were done within C_s point group in order to keep the same active space for all PESs despite the fact that more symmetric configurations were used. The second and fifth columns of the Table 1 contain information about the electronic wave function classification for a given geometric symmetry.

Finally, in Table 2 we present a comparison of atomization energies for the nine lowest electronic states calculated by the DIM and ab initio methods. For each state the geometries have been optimized at the DIM level and the ab initio energies calculated by the scheme proposed in Sect. 1, i.e., the ground state has first been calculated using RCCSD-T with the *extended* basis set and then the excitation energies are obtained from the the icMRCI calculations with *reduced* basis set. For the completeness, the

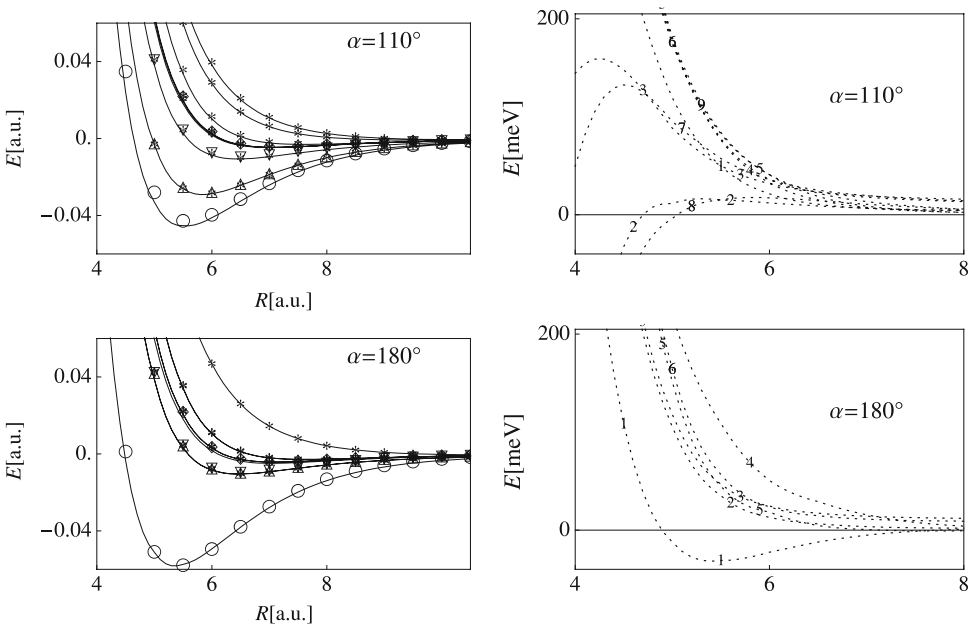

Fig. 8 Left column: Cuts through the PESs for Kr_3^+ at C_{2v} ($\alpha = 110°$) and linear symmetric nuclear configurations. Symbols correspond to ab initio data constructed from the ground state (RCCSD-T) PES with the icMRCI (*reduced* basis set) excitation energies. *Lines* correspond to the DIM data. Right column: *Dotted lines* are interpolations of differences between the nine and six ab initio and DIM PESs in meV (marked by the state numbers)

Table 1 Positive charge delocalization (central atom − wing atoms) and electronic wave function symmetry for nine lowest electronic states of Kr_3^+ at selected isosceles geometries ($R_{12} = R_{23} = 5.5$ a.u.)

The Mulliken population analysis has been used to process the icMRCI (*reduced* basis set) data

State No.	$\alpha = 180°$			$\alpha = 110°$		
	Symmetry	DIM	icMRCI	Symmetry	DIM	icMRCI
1	Σ_u^-	0.52–0.24	0.50–0.25	B_2	0.52–0.24	0.50–0.25
2	Π_u	0.54–0.23	0.56–0.22	A_1	0.52–0.24	0.50–0.25
3	Π_u	0.54–0.23	0.56–0.22	B_1	0.56–0.22	0.56–0.22
4	Σ_g^-	0.00–0.50	0.01–0.48	B_2	0.00–0.50	0.00–0.50
5	Π_g	0.00–0.50	0.01–0.48	A_2	0.00–0.50	0.00–0.50
6	Π_g	0.00–0.50	0.03–0.48	A_1	0.00–0.50	0.00–0.50
7	Π_u	0.46–0.27	0.42–0.29	B_1	0.44–0.28	0.40–0.30
8	Π_u	0.46–0.27	0.42–0.29	A_1	0.48–0.26	0.46–0.27
9	Σ_u^-	0.48–0.26	0.46–0.27	B_2	0.48–0.26	0.46–0.27

Table 2 Equilibrium geometries and atomization energies for the nine lowest electronic states of Kr_3^+ for the spin–orbit coupling and the zero-point energy not included

State		Geometry	Charges (1–2–3)	Energy	
				DIM	RCCSD-T + Δ icMRCI
1	$D_{\infty h}$	$r_{12} = r_{23} = 2.846$	0.24–0.52–0.24	1.575	1.605
2*	C_{2v}	$r_{12} = r_{23} = 3.007$, $\alpha_{123} = 84$	0.24–0.52–0.24	1.027	0.959
3	D_{3h}	$r_{12} = r_{23} = r_{13} = 3.255$	0.33–0.33–0.33	0.671	0.620
4	C_{2v}	$r_{12} = r_{23} = 3.783$, $\alpha_{123} = 52$	0.50–0.00–0.50	0.307	0.272
5*	D_{3h}	$r_{12} = r_{23} = r_{13} = 3.587$	0.33–0.33–0.33	0.274	0.240
6	C_{2v}	$r_{12} = r_{23} = 3.764$, $\alpha_{123} = 92$	0.50–0.00–0.50	0.126	0.116
7*	C_{2v}	$r_{12} = r_{23} = 3.973$, $\alpha_{123} = 72$	0.42–0.16–0.42	0.104	0.085
8*	$D_{\infty h}$	$r_{12} = r_{23} = 4.040$	0.38–0.24–0.38	0.077	0.067
9	D_{3h}	$r_{12} = r_{23} = r_{13} = 5.717$	0.33–0.33–0.33	0.025	0.022

The geometries have been optimized at the DIM level and the ab initio energies calculated for these optimized geometries using the RCCSD-T ground state and the icMRCI (*reduces* basis set) excitation energies

The energies correlate asymptotically to $Kr^+(^2P) + Kr(^1S) + Kr(^1S)$

All energies are given in eV, distances in Å, angles in degrees and charges in multiples of the elementary charge. Note that the states marked with stars intersect at the specified geometry with adjacent lower state at the DIM level

equilibrium positions and ionization energies obtained by the DIM + SO approach are given in Table 3.

4.3 Spin–orbit interaction

For krypton, the spin–orbit interaction must be considered in realistic models that reproduce or predict spectroscopic data. Similarly, as for the ground state RCCSD-T energies, the SO coupling has been included in the icMRCI data through a semi-empirical approach. First, the DIM Hamiltonian (without the inclusion of SO) has been diagonalized and resulting eigenvectors subsequently used to convert adiabatic icMRCI energies into the diabatic terms corresponding to the diabatic basis set employed in the DIM models. As the differences between the DIM and the icMRCI energies can be considered as a small perturbation, this procedure is accurate up to the first order of the perturbation theory. Second, the resulting icMRCI

Table 3 Equilibrium geometries and atomization energies for the nine lowest electronic states of Kr_3^+ with the spin–orbit coupling included and calculated at the DIM + SO level

State	Geometry		Charges (1–2–3)	Energy
1	$D_{\infty h}$	$r_{12} = r_{23} = 2.854$	0.24–0.52–0.24	1.386
2	C_{2v}	$r_{12} = r_{23} = 3.027$, $\alpha_{123} = 85$	0.26–0.48–0.26	0.723
3	D_{3h}	$r_{12} = r_{23} = r_{13} = 3.291$	0.33–0.33–0.33	0.544
4	D_{3h}	$r_{12} = r_{23} = r_{13} = 3.709$	0.33–0.33–0.33	0.180
5	$D_{\infty h}$	$r_{12} = r_{23} = 4.040$	0.38–0.24–0.38	0.077
6*	D_{3h}	$r_{12} = r_{23} = r_{13} = 3.973$	0.33–0.33–0.33	0.045
7	D_{3h}	$r_{12} = r_{23} = r_{13} = 3.818$	0.33–0.33–0.33	0.273
8	$D_{\infty h}$	$r_{12} = r_{23} = 3.753$	0.50–0.00–0.50	0.120
9	D_{3h}	$r_{12} = r_{23} = r_{13} = 4.427$	0.33–0.33–0.33	0.085

The energies do not include the zero-point vibration contributions and correlate asymptotically to $Kr^+(^2P_{3/2}) + Kr(^1S_0) + Kr(^1S_0)$ for states 1–6 and to $Kr^+(^2P_{1/2}) + Kr(^1S_0) + Kr(^1S_0)$ for states 7–9

The units used are as in Table 2. Note that the state marked with star intersects at the specified geometry with adjacent lower state at the DIM + SO level

Table 4 Evaporation energies (in eV) for $Kr_3^+(D_{\infty h}) \rightarrow Kr_2^+ + Kr$, both Kr_3^+ and Kr_2^+ in the ground electronic state, a comparison of the theory with experiments

Method	Energy
Exp. Ref. [36]	0.229 ± 0.007
Exp. Ref. [37]	0.27
DIM + SO	0.234 (0.238)
DIM + SO + ID–ID	0.240 (0.245)
RCCSD-T + SO (Eq. 2)	(0.246)

Theoretical values given in parentheses do not include the zero point energies

Hamiltonian matrix has been augmented by the SO terms as described in Ref. [12] and diagonalized. The eigenvalues provided by this last diagonalization represent, up to the first order of perturbation theory, the icMRCI energies with the SO coupling included. The cuts through the potential energy surfaces including SO presented in Fig. 9 illustrate a satisfactory agreement of the ab initio and extended semi-empirical DIM model [4]. The DIM–ab intio energy differences are identical as in the spin-free case in Fig. 8. Inclusion of the spin–orbit interaction makes possible a comparison of our results with available experiments. Data presented in Table 4 also confirms good performance of the DIM + SO, DIM + SO + ID–ID (the DIM + SO model with the inclusion of the

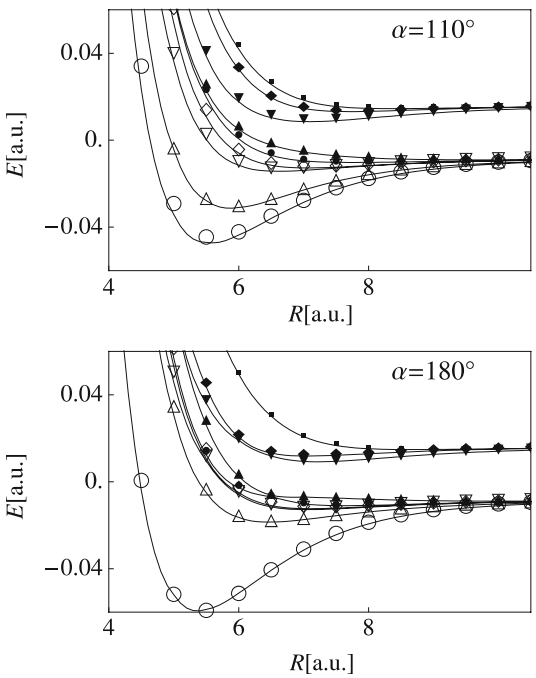

Fig. 9 Illustration of the overall agreement of the electronic potential energies of Kr_3^+ obtained by the DIM+SO model (*lines*) and by the ab initio (*symbols*) calculations (ground state from RCCSD-T with *extended* basis set, excitation energies from icMRCI with *reduced* basis set) in C_{2v} ($\alpha = 110°$) and linear symmetric arrangements

polarization three-body forces from Ref. [4]), and ab initio approaches.

5 Conclusions and outlook

The potential energy surfaces for all the electronic states of Kr_3^+ dissociating to $Kr(^1S) + Kr(^1S) + Kr^+(^2P)$ have been calculated for a large range of nuclear configurations using the RCCSD-T and icMRCI correlation methods and *extended* and *reduced* basis sets of Gaussian atomic orbitals, (10s8p6d6f2g)/[8s6p6d6f2g] and (8s8p3d1f1g)/[6s6p3d1f1g], respectively. The RCCSD-T calculations with the *extended* basis set provide highly accurate potential energy surfaces for the electronic ground state of particular wave function symmetries of Kr_3^+. The PESs for the B_2 and A_1 states at the C_{2v} symmetry were calculated over a large range of nuclear configurations. The spin–orbit coupling was successfully incorporated via a semi-empirical scheme. Multiconfigurational (icMRCI) calculations with the *extended* basis were carried on for the nine lowest electronic states of Kr_3^+ at selected C_{2v} nuclear configurations. The general agreement of these accurate PESs and semi-empirical DIM data justifies the use of the DIM models [4, 5, 13, 26, 27] and, consequently, their extension to larger clusters in theoretical studies. The DIM approach works remarkably well compared to the sophisticated ab initio calculations. Such accurate ab initio calculations are, however, meaningful if one needs to check the model, e.g. in the regions of strong interaction. We have shown, that passing from the *extended* to a *reduced* basis set in the multi-root calculation substantially reduces computing demands, while leaving the transition energies almost unchanged. The use of these excitation energies together with the highly accurate ground state RCCSD-T energies and the semi-empirical spin–orbit contributions is now the most feasible way towards reliable PESs of Kr_3^+ in a wide interval of nuclear configurations. They could be represented analytically and used eventually for refining the semi-empirical models (e.g., adiabatic ionization energies) for spectroscopic studies. Progressing in this direction, we have calculated the ground and excited states ab initio PESs at the vicinity of the equilibrium geometry of the neutral Kr_3 complex (equilateral arrangement, $R_e = 7$ a.u.), i.e., at the region where the knowledge of potential energies surfaces of all possible states can be especially helpful for photoelectron spectroscopy experiments [10]. We have found a very good agreement with the DIM model results. The ab initio data are available on request. Work is in progress to evaluate the spin–orbit contributions for the dimer and trimer krypton ions with an ab initio approach.

Acknowledgments This work was supported by the Grant Agency of the Academy of Sciences of the Czech Republic grant no. IAA100400501. Calculations were performed using computational facilities of the J. Heyrovský Institute and the Center of Numerically Demanding Calculations of University of Ostrava (financially supported by the Ministry of Education, Youth, and Sports of the Czech Republic, grant No. 1N04125). One of us (RK) acknowledges partial financial support from the University of Ostrava through the Foundation for Support of R&D Centers. Authors thank to Dr. R. Polák for helpful discussions of ab initio calculations and wave functions analysis.

References

1. Holland H (ed) (1994) Clusters of atoms and molecules. Springer Series in Chem Phys 52, Springer, Heidelberg
2. Kuntz P, Valldorf J (1988) Z Phys D 8:195
3. Galindez J, Calvo F, Paška P, Hrivňák D, Kalus R, Gadea FX (2002) Comp Phys Commun 145:126
4. Kalus R, Paidarová I, Hrivňák D, Paška P, Gadea FX (2003) Chem Phys 294:141
5. Hrivňák D, Kalus R, Gadea FX (2005) Europhys Lett 71:42
6. Naumkin FY, Knowles P, Murrell JN (1995) Chem Phys 193:27
7. Ritschel T, Kuntz PJ, Zülicke L (2005) Eur Phys J D 33:421
8. Ritschel T, Zuhrt C, Zülicke L, Kuntz PJ (2007) Eur Phys J D 41:127
9. Ritschel T, Kuntz PJ, Zülicke L (2007) Eur Phys J D 44:93
10. Willitisch S, Wüest A, Merkt F (2004) Chimia 58:281
11. Ellison FO (1963) J Am Chem Soc 85:3540
12. Amarouche M, Durand G, Malrieu JP (1988) J Chem Phys 88:1010
13. Kalus R, Paidarová I, Hrivňák D, Gadea FX (2004) Chem Phys 298:155
14. Kalus R, Hrivňák D (2004) Chem Phys 303:279
15. Kalus R, Hrivňák D, Vítek A (2006) Chem Phys 325:278
16. Cohen J, Schneider B (1974) J Chem Phys 61:3230
17. Dham AK, Allnatt AR, Meath WJ, Aziz RA (1989) Mol Phys 67:1291
18. Sugar J, Musgrove A (1991) J Phys Chem Ref Data 20:859
19. Hohm U, Kerl K (1990) Mol Phys 69:803
20. Knowles PJ, Hampel C, Werner HJ (1993) J Chem Phys 99:5219
21. Deegan M, Knowles P (1994) Chem Phys Lett 227:321
22. Nagata T, Hirokawa J, Kondow T (1991) Chem Phys Letters 176:526
23. Werner HJ, Knowles PJ, Lindh R, Manby FR, Schütz M, Celani P, Korona T, Rauhut G, Amos RD, Bernhardsson A, Berning A, Cooper DL, Deegan MJO, Dobbyn AJ, Eckert F, Hampel C, Hetzer G, Lloyd AW, McNicholas SJ, Meyer W, Mura ME, Nicklass A, Palmieri P, Pitzer R, Schumann U, Stoll H, Stone AJ, Tarroni R, Thorsteinsson T (2006) Molpro 2006 1 a package of ab initio programs. Available at http://www molpro net/
24. Nicklass A, Dolg M, Stoll H, Preuss H (1995) J Chem Phys 102:8942
25. Paidarová I, Gadea FX (2001) Chem Phys 274:1
26. Janeček I, Hrivňák D, Kalus R, Gadea FX (2006) J Chem Phys 125:104315
27. Hrivňák D, Kalus R, Gadea FX (2009) Phys Rev A 79:013424
28. Haberland H, von Issendorf B, Hofmann A (1995) J Chem Phys 103:3450
29. Werner HJ, Knowles P (1988) J Chem Phys 89:5803
30. Knowles P, Werner HJ (1988) Chem Phys Lett 145:514
31. Langhoff SR, Davidson ER (1974) Int J Quant Chem 8:61
32. Blomberg MRA, Siegbahn PEM (1983) J Chem Phys 78:5682
33. Knowles P, Werner HJ (1985) Chem Phys Lett 115:259
34. Werner HJ, Knowles P (1985) J Chem Phys 82:5053
35. Gadea FX, Paidarová I (1996) Chem Phys 209:281
36. Hiraoka K, Mori T (1990) J Chem Phys 92:4408
37. Fehsenfeld F, Brown T, Albritton D (1978) Evaporation energies of Kr3. In: Proceedings of the 31st gaseous electronics conference, Buffalo, 1978